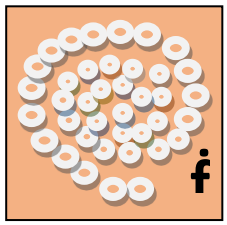

International Journal of Mathematical Analysis and Modelling

(Formerly Journal of the Nigerian Society for Mathematical Biology)

Volume 8 Issue 1, 2025

ISSN (Print): 2682 - 5694
ISSN (Online): 2682 – 5708
www.tnsmb.org

Sensitivity and stability analyses of COVID-19 model with waning immunity and relapse: a case study of Nigeria

M.O. Ogunmodimu[*†], **T.T. Yusuf**[†‡], and **O. Olotu**[†§]

Abstract

The Coronavirus Disease 2019 (COVID-19) experienced an exponential increase in cases between October 2023 and January 2024, with a growth factor of 6.53, following a period of gradual decline in previous years. Nigeria, a densely populated developing country in Africa with limited preparedness for epidemics, was caught unawares by this sudden re-emergence. This study investigates COVID-19 re-infections among individuals who had previously recovered or had been vaccinated, using Nigeria as case study. A deterministic compartmental model capturing the transmission, prevention, and control dynamics of COVID-19 was developed. The qualitative properties of the model, namely positivity and boundedness of its solutions, were established. Stability analysis of the model's equilibria was conducted by deriving and analyzing the effective reproduction number, R_e. The model was shown to exhibit a stable disease-free equilibrium when $R_e < 1$ and a unique globally stable endemic equilibrium when $R_e > 1$. Sensitivity analysis of R_e was carried out by employing the forward index sensitivity approach. The results indicated that recruitment into the susceptible population and contact rate have unit sensitivity indices. Waning immunity of the vaccinated class was shown to have a direct relationship with R_e, resulting in re-infections, whereas vaccination and recovery rates have an inverse relationship. Numerical simulations were conducted using the fourth-order Runge-Kutta method implemented via a MATLAB subroutine. Model parameters were estimated using data from the Nigeria Centre for Disease Control (NCDC) and weekly trends of the COVID-19 pandemic. Each parameter sensitive to R_e was varied and their effect on the re-emergence of infection discussed. Results indicated that disease prevalence increases with higher rates of relapse, contact, and recruitment into the susceptible population and decreases with higher rates of treatment and vaccination.

Keywords and phrases: COVID-19; Disease Relapse; Sensitivity Analysis; Stability Analysis; Waning Immunity.

1 Introduction

Human history bears the lasting imprint of the influence of infectious diseases. Several past epidemics have affected large populations, resulting in high mortality rates. The Spanish flu epidemic of 1918–1919 led to over 50 million deaths worldwide [1]. The Black Death, caused by the Yersinia pestis bacterium and also known as the Bubonic Plague, originated in Asia and swept through Europe in the 14th century in several waves [2]. This disease was estimated to have caused the death of one-third of the population of Europe between 1346 and 1350, lasted for atleast 300 years, later to be called "the Great Plague of London of 1665–1666". Meanwhile, there are also diseases that have become always present (endemic) in some populations causing many deaths just as there are annual influenza seasonal epidemics that cause up to 35,000 deaths worldwide [1].

In late December 2019, a viral respiratory disease, later identified on January 9, 2020 as Coronavirus Disease 2019 (COVID-19), emerged in Wuhan, China. The disease, caused by the novel Severe Acute

[*]Corresponding Author; E-mail: akinademary18@gmail.com, ORCID: 0000-0002-3159-2155
[†]Department of Mathematical Sciences, The Federal University of Technology, Akure, Ondo State, Nigeria
[‡]E-mail: ttyusuf@futa.edu.ng
[§]E-mail: oolotu@futa.edu.ng

Respiratory Syndrome Coronavirus 2 (SARS-CoV-2), was believed to have spilled over from animals to humans in a live animal market [3]. The SARS-CoV-2 was reported to have spilled over from animals to humans in a big market that sold live animals, among other goods, in Wuhan. From that time onward, COVID-19 has continued to spread among human-population when an individual comes in close direct contact with an infected person, with respiratory droplets of such or with contaminated objects and surfaces. At the onset of infection, the SARS-CoV-2 is established in the respiratory tract and especially the upper respiratory tract (URT) consisting of the nose and throat.

The incubation period of COVID-19, the period between exposure to the disease and onset of symptoms, ranges from 5 to 14 days. During this period, some individuals may recover through their natural immune response without ever realizing they were infected while others may become contagious while being asymptomatic before progressing to a full state of symptomatic infectiousness. While most people infected with COVID-19 only develop mild symptoms such as cough, tiredness, shortness of breath or difficulty in breathing, similar to that of common cold and fever, approximately 15% develop severe disease that requires oxygen support, and 5% have critical disease with complications such as respiratory failure, acute respiratory distress syndrome, etc [4].

Some risk factors for higher severity and consequently higher mortality rate for COVID-19 are pre-existing disease such as tuberculosis, hypertension, diabetes, obesity, cancer, people aged 60 and above, individuals that are not vaccinated against it, advanced maternal age for pregnant women, etc [5]. According to a report by [6], as of January 7, 2024, over 774 million cases of COVID-19 had been recorded worldwide, with over 7 million deaths. The death rate was highest during the first year of outbreak. On March 11, 2020, 3 months into the outbreak of the disease, WHO declared COVID-19 a global pandemic.

The WHO identifies with five variants of concern (VoC) for COVID-19, namely; Alpha, Beta, Gamma, Delta and Omicron (the most dominant variant with 15% death rate of infected individuals). It is however not defined if a VoC causes more severe disease or higher mortality, as many other factors are involved [7]. The treatment for mild and moderate cases of COVID-19 infection include: symptom management and supportive care, monitoring (via quarantine or hospitalization), over-the-counter medicines such as acetaminophen or ibuprofen, while patients with risk of progression to severe disease are treated with Ritonavir-boosted nirmatrelvir, Remdesivir and Molnupiravir [5].

There are quite a number of vaccines, with varying efficacy validated by the WHO against the COVID-19; the Pfizer/BioNTech Comirnaty, the Covovax (NVX-CoV2373), and the Nuvaxovid (NVX-CoV2373) vaccines. Moderna Spikevax, Oxford AstraZeneca, Janssen, Spunik V, Pfizer-BioNTech and Sinopharm BIBP are vaccines approved for use in Nigeria. The Oxford AstraZeneca vaccine came into Nigeria on February 18, 2021 and was first administered on March 5, 2021 [8]. The effectiveness of COVID-19 vaccine against infection and mild symptoms, however, can wane over time, the same way one can lose immunity and become re-infected with the disease after recovery. In addition to vaccination, the WHO recommends non-pharmaceutical preventive measures such as personal hygiene, contact tracing and isolation, partial/total lock-down, social distancing of at least 1 meter away from other people, wearing a properly fitted mask over the nose and mouth, avoiding poorly ventilated places and settings, etc, against the spread of COVID-19.

Although, some countries in the world have been able to manage and slow down infectiousness rate of SARS-Cov-2, the virus continues to spread in other communities and countries erratically. Most recently, a multi-system inflammatory syndrome temporally associated with COVID-19 in children and adolescents have been reported [9]. The partial easing of the COVID-19 induced lockdown in Nigeria in mid-2020 led to an approximately 60% rise in cases and a related 33% increase in reported deaths [10].

A live count of 4,035 COVID-19 cases were recorded on the 22nd December 2022 alone and 35 new cases in the last week of December 2022. On January 24 2024, there were 3,567 active COVID-19 cases in Nigeria and 22,076,9756 active cases in the world [11, 12]. As indicated in figure 1, as at April 3rd, 2024, there were 4,080 active COVID-19 cases in Nigeria and 22,204,908 in the world with a total of 704,753,890 cumulative cases (including deaths and recovered or discharged patients) in the

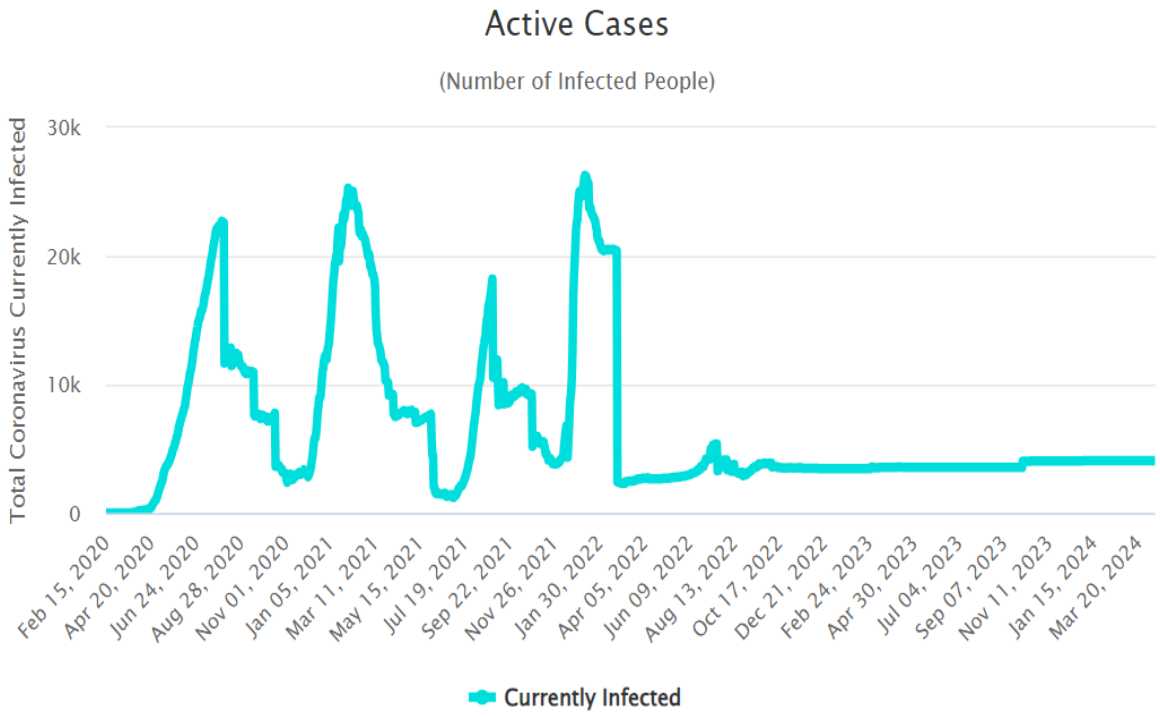

Figure 1: Active COVID-19 Cases in Nigeria: Feb. 2020 - April 2024 [13]

world as at April 13th, 2024 [13].

Figure 2 shows the growth factor of COVID-19 globally from 2020 to 2024 indicating an exponential increase between October 2023 and January 2024 and attaining a precarious growth factor of 6.53 on January 23rd 2024. This sudden increase in infectiousness signals a need for the development of a novel mathematical model to investigate this re-emergence of infections, possible causes and measures against it, hence this research work.

Growth factor is the factor by which a quantity multiplies itself over time. The formula used is every day's new cases divided by new cases on the previous day. For example, a quantity growing by 7% every period (in this case daily) has a growth factor of 1.07. A growth factor above 1 indicates an increase, whereas one which remains between 0 and 1 is a sign of decline, with the quantity eventually becoming zero, whereas a growth factor constantly above 1 could signal exponential growth.

Several studies have employed compartmental models such as SEIR frameworks to capture the transmission dynamics of COVID-19 [14, 15, 16, 17, 18]. However, many of these models either ignore the effects of waning immunity after vaccination or do not account for relapse after recovery. [19] developed a SEIR mathematical model to predict the possible epidemic peak and size of COVID-19 in Algeria. Using the method of least squares and the best fit curve, the basic reproduction number of the model was obtained as $R_0 = 4.1$. This implied that the outbreak in Algeria was strong and that the nation must implement strict measures, including a nationwide lockdown, similar to what was adopted in China.

Equally, [20] studied the transmission dynamics of an SEIR compartmental model for COVID-19 using two non-singular kernel fractional derivative operators. The basic reproduction number was obtained using the next generation matrix approach. The long-term possibilities of the infection were examined using the Caputo–Fabrizio (CF) and Atangana–Baleanu derivative in Caputo sense (ABC) models. The existence and uniqueness of solution were examined for these model extensions. Numerical simulations of the model were carried out using MATLAB for both the CF and the ABC method, and the results compared. The results obtained show that the CF approach can be used in modeling mild cases of infectious diseases while the ABC fractional derivative approach proves to be more effective in

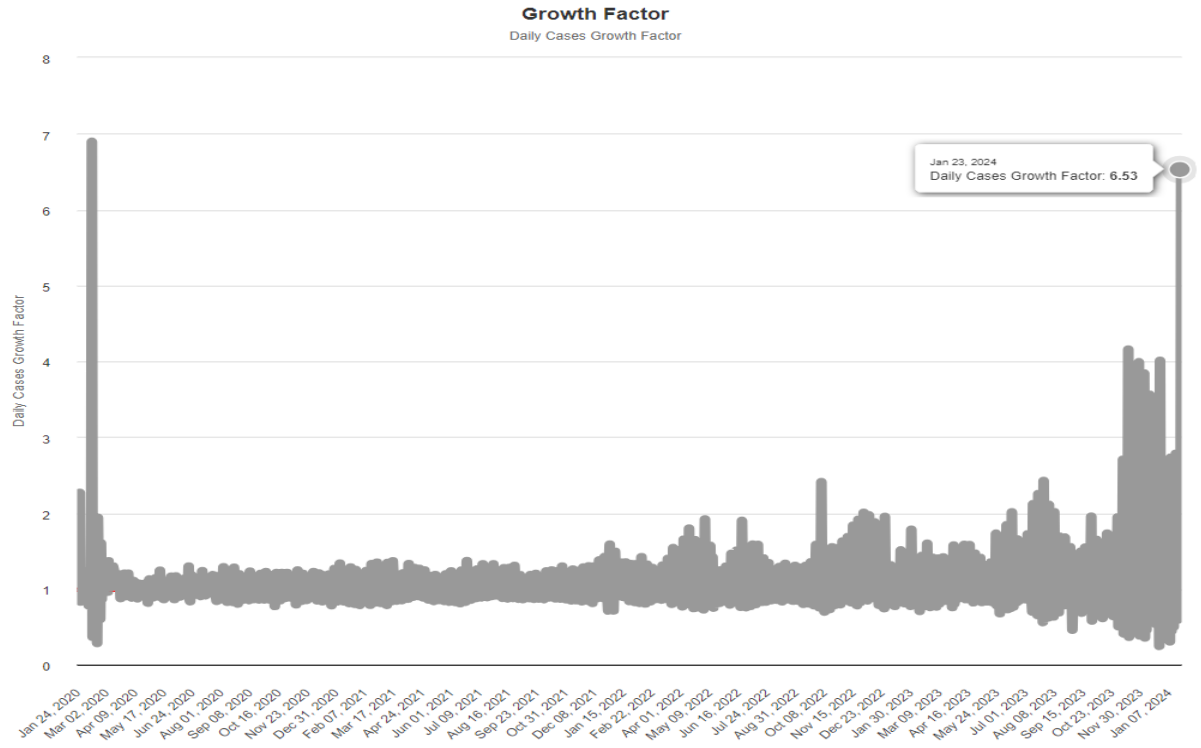

Figure 2: Growth Factor of Daily New Cases of COVID-19 Worldwide: Jan. 2020-Jan. 2024 [13]

modeling advance disease transmission dynamics including critical COVID-19 cases.

The effect of an "imported escaper" was considered by [21] in a model developed to fit an epidemic data collected between January 23rd and March 25th 2020 from the Heilongjiang province of China. The simulation performed showed that an imported 'escaper' was responsible for the newly confirmed COVID-19 infections from April 9th to April 19th 2020 in the province. It was also obtained that an implementation of stronger interventions to lower mutual contacts could accelerate the complete recovery from COVID-19 infections in the province.

In a similar study by [22], an eight-compartmental mathematical model to study the transmissibility of super-spreader individuals for COVID-19 using Wuhan, China, where the outbreak was first recorded, as case study was developed. The basic reproduction number, R_0, was obtained as 0.945 and the local stability of the DFE point established. Sensitivity analysis of R_0 was carried out and the result indicated that the transmission coefficient from infected individuals is the most sensitive parameter to the spread of the disease followed closely by the rate at which exposed people become infected. Numerical simulation was carried out using the MATLAB code ode45 algorithm and the results obtained reflected the reality in Wuhan.

Subsequently, [23] made a prediction on the epidemic peak of COVID-19 in Brazil at different transmission rates. The Predictor–Corrector (P-C) scheme was applied on the developed model and real-life data were used for its numerical simulation. The results of the simulation showed that an increase in the infection rate will result in the disease becoming more deadly and that there were a lot of uncertainties in the peak of COVID-19 in Brazil.

[24] considered the effect of an hypothetical imperfect vaccine on the control of COVID-19. Numerical analyses of their model indicated that individuals who are infected with the second strain of SARS-CoV-2 and are vaccinated with an imperfect vaccine are under control unlike those infected with the first strain. It was also obtained that the prevalence of the second strain enhances the prevalence of the first. This conclusion informs the need for the development of a model which will consider an efficacious vaccine for all strains of COVID-19.

Using Nigeria as case study, [25] developed a 5 compartmental non-linear ODE model to investi-

gate the imposition of lockdown during COVID-19 pandemic. Mathematical analyses of the model, including the boundedness of solutions, obtaining the equilibria, computation of the basic reproduction number and stability analysis of the equilibria, were performed. Numerical simulations were performed using the ODE45, Euler, RK-2 and RK-4 schemes and the results obtained from each scheme were compared using graphical representations. It was however recommended that the rest of the COVID-19 measures be studied and their significance analyzed.

Similarly, [26] developed a model to describe the dynamics of COVID-19, taking into cognizance its transmission route from quarantined individuals. The basic reproduction number of the model was estimated to be between 0.669 and 0.680, indicating that the spread of the disease was dwindling as at 2021. Parameters of the model were estimated from NCDC and the result of numerical simulation performed showed that recovery and transmission rates are most significant to the control of COVID-19. The research however did not consider the effect of vaccination on the spread of the disease. In this work, we considered vaccination of the susceptible population as a measure against the continuous transmission of the disease while also considering the effect of disease relapse and immunity wane on its spread.

Despite the several studies modeling the dynamics of COVID-19 globally and in Nigeria, limited attention has been paid to the role of immunity waning and relapse, especially in the context of post-vaccination reinfections. Given the recent surge in COVID-19 cases in Nigeria and the evidence of recurrent infections [10], it becomes imperative to develop a mathematical model that incorporates these factors. This work addresses that gap by constructing a deterministic model that considers both immunity waning and reinfection dynamics within the Nigerian context.

2 Model Formulation

In this research, we employed the compartmental disease modelling approach to develop an SIRV model for COVID-19 as a system of 4 ordinary differential equations corresponding to the susceptible $S(t)$, infected $I_C(t)$, recovered via treatment $R_C(t)$ and vaccinated $V_C(t)$ populations respectively. These populations are referred to as the model's state variables. Λ represents the recruitment rate into the susceptible population, μ represents the natural death rate of humans while δ_C represents the COVID-19 induced death rate. The transmission rate of COVID-19 is denoted by β_C and the disease is contracted by the susceptible and vaccinated populations only via the force of infection $\lambda_1 = \beta_C I_C$. The vaccination and recovery rates are ν_C and γ_C respectively. The vaccinated population losses there immunity at the rate ω_C and the disease relapse rate for the recovered population is denoted by θ_C. The flow diagram for the developed model is presented in figure 3 and the model parameters contained in table 1.

2.1 The COVID-19 Model

$$\frac{dS}{dt} = \Lambda - \nu_C S - \lambda_1 S + \omega_C V_C + \theta_C R_C - \mu S, \tag{1}$$

$$\frac{dI_C}{dt} = \lambda_1 S - \gamma_C I_C - (\delta_C + \mu) I_C, \tag{2}$$

$$\frac{dR_C}{dt} = \gamma_C I_C - \theta_C R_C - \mu R_C, \tag{3}$$

$$\frac{dV_C}{dt} = \nu_C S - \omega_C V_C - \mu V_C. \tag{4}$$

with initial conditions; $\{(S, I_C, R_C, V_C) \in R_+^4 : S_0 \geq 0, I_{C0} \geq 0, R_{C0} \geq 0, V_{C0} \geq 0\}$.

Table 1: Description of the Model's Parameters

Parameters	Description
Λ	Recruitment rate into the susceptible population by birth or immigration
μ	Natural death rate
δ_C	COVID-19 induced death rate
β_C	COVID-19 effectual transmission rate
λ_1	Force of infection associated with COVID-19
ν_C	COVID-19 vaccination rate
γ_C	COVID-19 recovery rate via treatment
ω_C	Rate of loss of immunity for the vaccinated class
θ_C	Rate of disease relapse for the recovered class

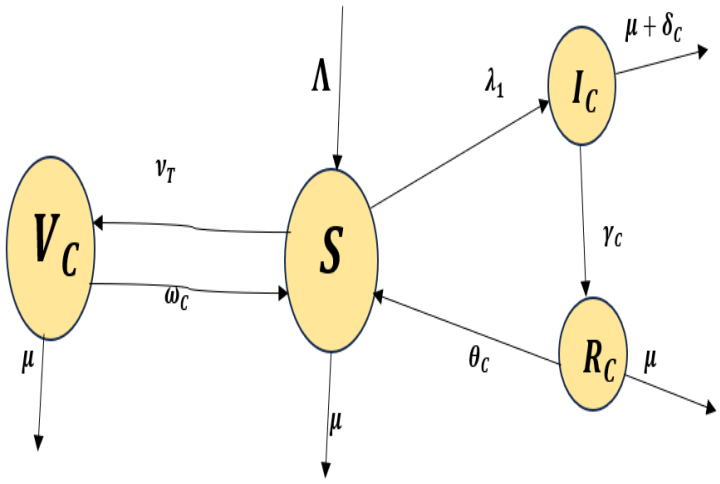

Figure 3: Flow Diagram for the COVID-19 Model

Assumptions of the Model

The following assumptions were made, without loss of generality, in the development of the model:

1. Each population in the model is mutually exclusive.
2. There exists effective treatment measure for COVID-19 and individuals under such are religious with it.
3. The recovered population are not infectious.
4. There is no escape from the treatment centre until full recovery.
5. Vaccination is given only to the susceptible population.

2.2 Qualitative Properties of the Model

Two qualitative properties of an epidemic model are presented and established in order to guarantee that the developed model is epidemiologically well posed.

2.2.1 The Invariant Region of Solution

To obtain the invariant region of the model, a bounded region in which the model's solution exists,

we define the total human population as the sum of the 4 mutually independent populations, that is;

$$N_C(t) = S(t) + I_C(t) + R_C(t) + V_C(t) \tag{5}$$

We then obtain the equation for the derivative of $N_C(t)$ with respect to t by adding all 4 equations of the model;

$$\begin{aligned} \frac{dN_C(t)}{dt} &= \Lambda - \mu N_C(t) - \delta_C I_C & (6)\\ &\leq \Lambda - \mu N_C(t) & (7)\end{aligned}$$

$$\therefore \int \frac{dN_C(t)}{\Lambda - \mu N_C(t)} \leq \int dt \tag{8}$$

$$\implies \frac{-1}{\mu}\ln(\Lambda - \mu N_C(t)) \leq t + C,$$

where C is a constant of integration.

Thus,

$$\ln(\Lambda - \mu N_C(t)) \geq -(\mu t + C)$$
$$\implies (\Lambda - \mu N_C(t)) \geq Ae^{-\mu t},$$

where $A = e^{-C}$ is a constant.

At $t = 0$, $N_C(0) = N_{C0} \geq 0$

$$\therefore (\Lambda - \mu N_{C0}) \geq A.$$

Accordingly,

$$(\Lambda - \mu N_C(t)) \geq (\Lambda - \mu N_{C0})e^{-\mu t}$$
$$-\mu N_C(t) \geq -\Lambda + (\Lambda - \mu N_{C0})e^{-\mu t}$$
$$\implies N_C(t) \leq \frac{\Lambda}{\mu} - \frac{(\Lambda - \mu N_{C0})}{\mu}e^{-\mu t}$$
$$\implies N_C(t) \to \frac{\Lambda}{\mu} \ as \ t \to \infty.$$

Thus, $N_C(t) \in [N_{C0}, \frac{\Lambda}{\mu}]$.

Hence, the feasible set of the solution of the COVID-19 model is bounded in the region:

$$\Omega = \{(S, I_C, R_C, V_C) \in R_+^4 : N_C(t) \leq \frac{\Lambda}{\mu}\} \tag{9}$$

2.2.2 Positivity of Solution

The positivity theorem [27] states that the solutions of a model's equations are positively invariant for future time if the respective initial values of the model's state variables are all non-negative". Let $\Omega_1 = \{(S, I_C, R_C, V_C) \in R_+^4 : (S_0 > 0, I_{C0} > 0, R_{C0} > 0, V_{C0} > 0)\}$, then the solution of $\{(S, I_C, R_C, V_C)\}$ are non negative for $t \geq 0$.

Proof: Considering equation (1),

$$\frac{dS}{dt} = \Lambda - \nu_C S - \lambda_1 S + \omega_C V_C + \theta_C R_C - \mu S$$
$$\geq -(\nu_C + \lambda_1 + \mu)S.$$
$$\int \frac{dS}{S} \geq -\int (\nu_C + \lambda_1 + \mu)dt$$
$$\ln S(t) \geq -A(t) + C$$

$$S(t) \geq Be^{-A(t)},$$

where $A(t) = \int(\nu_C + \lambda_1 + \mu)dt$, C is a constant of integration.

At $t = 0, S_0 > 0$

$\therefore S(t = 0) = S_0 \geq B$

$$\begin{aligned} S(t) &\geq S_0 e^{-A(t)} \\ &\geq 0 \qquad \forall\, t > 0. \end{aligned} \tag{10}$$

Considering equation (2),

$$\begin{aligned} \frac{dI_C}{dt} &= \lambda_1 S - \gamma_C I_C - (\delta_C + \mu) I_C \\ &\geq -(\gamma_C + \delta_C + \mu) I_C. \end{aligned}$$

Thus,

$$\begin{aligned} \int \frac{dI_C}{I_C} &\geq -\int (\gamma_C + \delta_C + \mu)dt \\ \ln I_C(t) &\geq -A(t) + C \\ I_C(t) &\geq Be^{-A(t)}, \end{aligned}$$

where $A(t) = \int(\gamma_C + \delta_C + \mu)dt$, C is a constant of integration and $B = e^C$.

At $t = 0, I_{C0} > 0$

$\therefore I_C(t = 0) = I_{C0} \geq B$

Accordingly;

$$\begin{aligned} I_C(t) &\geq I_{C0} e^{-A(t)} \\ &\geq 0 \qquad \forall\, t > 0. \end{aligned} \tag{11}$$

Considering equation (3),

$$\begin{aligned} \frac{dR_C}{dt} &= \gamma_C I_C - \theta_C R_C - \mu R_C \\ &\geq -(\theta_C + \mu) R_C \end{aligned}$$

thus,

$$\begin{aligned} \int \frac{dR_C}{R_C} &\geq -\int (\theta_C + \mu)dt \\ \ln R_C(t) &\geq -A(t) + C \\ R_C(t) &\geq Be^{-A(t)}, \end{aligned}$$

where $A(t) = \int(\theta_C + \mu)dt$, C is a constant of integration and $B = e^C$.

At $t = 0, R_{C0} > 0$

$\therefore R_C(t = 0) = R_{C0} \geq B.$

Accordingly;

$$\begin{aligned} R_C(t) &\geq R_{C0} e^{-A(t)} \\ &\geq 0 \qquad \forall\, t > 0. \end{aligned} \tag{12}$$

Lastly, considering equation (4),

$$\begin{aligned} \frac{dV_C}{dt} &= \nu_C S - \omega_C V_C - \mu V_C \\ &\geq -(\omega_C + \mu) V_C. \end{aligned}$$

Thus,

$$\begin{aligned} \int \frac{dV_C}{V_C} &\geq -\int (\omega_C + \mu)dt \\ \ln V_C(t) &\geq -A(t) + C \end{aligned}$$

$$V_C(t) \geq Be^{-A(t)},$$

where $A(t) = \int(\omega_C + \mu)dt$, C is a constant of integration and $B = e^C$.

At $t = 0, V_{C0} > 0$

$\therefore V_C(t = 0) = V_{C0} \geq B$

Accordingly;

$$V_C(t) \geq V_{C0}e^{-A(t)} \geq 0 \qquad \forall\, t > 0. \tag{13}$$

2.3 Parameter Estimation

The model parameter values were estimated based on real data-sets of COVID-19 in Nigeria according to the Nigeria Centre for Disease Control and Prevention [11] and Corona virus pandemic weekly trends [13]. The average life expectancy (ALE) of Nigerians for the year 2024 is 56.05 [28]. Hence, the natural death rate of individuals was calculated by taking the reciprocal of the ALE (in weeks), that is;

$$\mu = \frac{1}{56.05 \times 52} = 0.0003431$$

The disease induced death rate = $\frac{totaldeath}{totalcases}$ [13] $= \frac{3155}{267188} = 0.01180817$
The treatment rate = $\frac{totaltreated}{totalcases}$ [11] $= \frac{3}{5} = 0.6$
The recruitment rate (by birth or immigration) is the ratio of the population growth to total population = $\frac{5,347,585}{229,152,217}$ [11] $= 0.023336$

Accordingly, the values of the model parameters are presented in table 2.

Table 2: Table of Values for the Model's Parameters

Parameters	Values	Sources
Λ	0.0233363	Estimated
μ	0.0003431	Estimated
δ_C	0.0118081	Estimated
β_C	0.0005944	[8]
ν_C	0.20	Assumed
γ_C	0.60	Estimated
ω_C	0.050	[8]
θ_C	0.010	[8]

3 Stability and Sensitivity Analyses of the Model

3.1 Disease Free Equilibrium (DFE)

A disease free equilibrium is a state in which a studied population remains in the absence of the disease(s). This imply that there are no infections nor recovery. Mathematically, the disease free equilibrium point of a model is obtained by analyzing the models' parameters at the point where the population remains in the absence of the disease.

We define the DFE of the developed model as:

$$E_{C0} = (S^*, 0, 0, V_C^*),$$

satisfying $\frac{dS}{dt} = \frac{dI_C}{dt} = \frac{dR_C}{dt} = \frac{dV_C}{dt} = 0$ and $I_C = R_C = 0$.

By equating equations (1)) to (4) to 0 and substituting $I_C = R_C = 0$, we have;

$$\frac{dS}{dt} = \Lambda - \nu_C S + \omega_C V_C + \theta_C R_C - \mu S = 0, \tag{14}$$

$$\frac{dV_C}{dt} = \nu_C S - \omega_C V_C - \mu V_C = 0. \tag{15}$$

The addition of equations (14) and (15) yields:

$$V_C = \frac{(\Lambda - \mu S)}{\mu}. \tag{16}$$

Substituting (16) in (14) yields:

$$\Lambda - (\nu_C + \mu + \omega_C)S + \Lambda\frac{\omega_C}{\mu} = 0,$$

$$\implies S^* = \frac{\Lambda}{\mu}H. \tag{17}$$

Where

$$H = \frac{(\mu + \omega_C)}{(\mu + \omega_C + \nu_C)}. \tag{18}$$

Substituting (17) in (16), we have;

$$V_C^* = \frac{\Lambda}{\mu}H^*, \tag{19}$$

where $H^* = (1 - H)$.

Therefore;

$$E_{C0} = (\frac{\Lambda}{\mu}H, 0, 0, \frac{\Lambda}{\mu}H^*). \tag{20}$$

Note that, $S^* = \frac{\Lambda}{\mu}$ iff $H = 1$ and this $\implies \nu_C = 0$ and $V_C = 0$.

3.2 Local Stability Analysis of the DFE

By evaluating the Jacobian (for non-linear systems) or coefficient matrix of a linear system of equations at an equilibrium point, the eigenvalues and behavior of such system in the neighborhood of that equilibrium point can be quantitatively determined. This method is referred to as the Routh-Hurwitz Stability criterion and it states that, "if all the eigen values of a system ae negative or have negative real part at an equilibrium point, then such point is locally asymptotically stable" [29, 30].

Another common method used in evaluating stability of DFE points is [8, 26, 31, 32, 33]. In epidemiology, this method is used to derive the basic reproduction number, R_0, for a compartmental model for the spread of infectious diseases. R_0 is the spectral radius of the next generation matrix FV^{-1} of the system. For a population that is not entirely susceptible, as in our model in which there exists a vaccinated population, we analyze the effective reproduction number, $R_e = R_0 X$, instead of R_0 for stability where X is the fraction of the population that is susceptible. If $R_e < 1$, then the DFE is locally asymptotically stable and unstable otherwise.

By employing the principle of Next Generation Matrix on the model, we define the rate of appearance of new infection, f_i, and the rate of transfer of individuals into compartments i in the model equations (1) to (4) as:

$$f_i - v_i = \begin{pmatrix} I_C' \\ R_C' \end{pmatrix}$$

$$= \begin{pmatrix} \beta_C I_C S^* - (\gamma_C + \delta_C + \mu)I_C \\ \gamma_C I_C - (\theta_C + \mu)R_C \end{pmatrix}$$

Accordingly; $f_i = \begin{pmatrix} \beta_C I_C S^* \\ 0 \end{pmatrix}$ and $v_i = \begin{pmatrix} (\gamma_C + \delta_C + \mu)I_C \\ (\theta_C + \mu)R_C - \gamma_C I_C. \end{pmatrix}$

Therefore, $F = \begin{pmatrix} \frac{\partial f_1}{\partial I_C} & \frac{\partial f_1}{\partial R_C} \\ \frac{\partial f_2}{\partial I_C} & \frac{\partial f_2}{\partial R_C} \end{pmatrix} = \begin{pmatrix} \beta_C S^* & 0 \\ 0 & 0 \end{pmatrix}$

and $V = \begin{pmatrix} \frac{\partial v_1}{\partial I_C} & \frac{\partial v_1}{\partial R_C} \\ \frac{\partial v_2}{\partial I_C} & \frac{\partial v_2}{\partial R_C} \end{pmatrix} = \begin{pmatrix} (\gamma_C + \delta_C + \mu) & 0 \\ -\gamma_C & (\theta_C + \mu). \end{pmatrix}$

Hence,

$$V^{-1} = \frac{1}{|V|} \begin{pmatrix} (\theta_C + \mu) & -\gamma_C \\ 0 & (\gamma_C + \delta_C + \mu) \end{pmatrix}$$

and the next generation matrix,

$$G = FV^{-1} = \begin{pmatrix} \frac{\beta_C S^*}{(\gamma_C + \delta_C + \mu)} & 0 \\ 0 & 0. \end{pmatrix}$$

The eigen values of the Matrix G are $[0, \frac{\beta_C S^*}{(\gamma_C + \delta_C + \mu)}]$.

Hence, the spectral radius of G, which is the maximum eigenvalue of G is :

$$\begin{aligned} R_0^C &= \frac{\beta_C S^*}{(\gamma_C + \delta_C + \mu)} \\ &= \frac{\frac{\Lambda}{\mu} H \beta_C}{(\gamma_C + \delta_C + \mu)} \\ &= \frac{\Lambda \beta_C (\mu + \omega_C)}{\mu(\mu + \omega_C + \nu_C)(\gamma_C + \delta_C + \mu)} \end{aligned} \tag{21}$$

by substituting S^* from (17) and H from (18) respectively.

Let X, the percentage of the population that is susceptible be $\frac{70}{100}$, then by substituting the parameter values in table 2, we obtain $R_0 = 0.51453625$ and the effective reproduction number of the model is:

$$R_e = R_0^C X = 0.36017537 \tag{22}$$

According to the principle of Next Generation Matrix, since the effective reproduction number is less than unity, then the DFE of the model is stable.

Routh Hurwitz Stability Criterion

We verified the above result by implementing the Routh Hurwitz Stability Criterion earlier discussed. In control system theory, the Routh–Hurwitz stability criterion is a mathematical test that is a necessary and sufficient condition for the stability of a linear time invariant (LTI) control system.

We define the Jacobian matrix of the system (1) to (4) at the DFE $E_{C0} = (S^*, 0, 0, V_C^*)$ as:

$$J = \begin{pmatrix} \frac{dj_1}{dS} & \frac{dj_1}{dI_C} & \frac{dj_1}{dR_C} & \frac{dj_1}{dV_C} \\ \frac{dj_2}{dS} & \frac{dj_2}{dI_C} & \frac{dj_2}{dR_C} & \frac{dj_2}{dV_C} \\ \frac{dj_3}{dS} & \frac{dj_3}{dI_C} & \frac{dj_3}{dR_C} & \frac{dj_3}{dV_C} \\ \frac{dj_4}{dS} & \frac{dj_4}{dI_C} & \frac{dj_4}{dR_C} & \frac{dj_4}{dV_C} \end{pmatrix}$$

$$= \begin{pmatrix} -(\mu + \nu_C) & -\beta_C S^* & \theta_C & \omega_C \\ 0 & \beta_C S^* - (\gamma_C + \delta_C + \mu) & 0 & 0 \\ 0 & \gamma_C & -(\mu + \theta_C) & 0 \\ \nu_C & 0 & 0 & -(\mu + \omega_C) \end{pmatrix}$$

The equilibrium point $E_{C0} = (S^*, 0, 0, V_C^*)$ is stable, iff all the eigen values of J are negative or complex with negative real parts.

The eigenvalues of the matrix J are $[-\mu, -(\mu + \theta_C), -(\mu + \omega_C + \nu_C), \beta_C S^* - (\gamma_C + \delta_C + \mu)]$ Clearly, all the eigenvalues of J are negative iff $\beta_C S^* - (\gamma_C + \delta_C + \mu) < 0$

$$\implies \frac{\beta_C S^*}{(\gamma_C + \delta_C + \mu)} < 1$$

Recall that $R_0^C = \frac{\beta_C S^*}{(\gamma_C + \delta_C + \mu)}$ from (21). By the Routh-Hurwitz stability criterion, the DFE of the COVID-19 model is stable whenever $R_0^C < 1, \implies R_e < 1$.

3.3 Global Stability Analysis of the DFE Point

In order to examine the DFE solution of the model for global stability, this guarantees the stability of the DFE irrespective of the initial size of the population, we employed the generalized method of constructing Lyapunov functions given by [34].

We constructed an appropriate Lyapunov function, V_C, for the model as the combination of the model's infected compartment. Thus we defined V_C as:

$V_C(t, S, I_C, R_C, V_C) = C_1 I_C; \;\; C_1 > 0.$

$$\begin{aligned} \frac{dV_C}{dt} &= C_1 I_C' \\ &= C_1(\beta_C I_C S - (\gamma_C + \delta_C + \mu) I_C) \\ &= C_1(\beta_C S - (\gamma_C + \delta_C + \mu)) I_C \\ &< 0; \quad R_0^C < 1 \implies \beta_C S - (\gamma_C + \delta_C + \mu) < 0 \end{aligned}$$

Recall R_0^C from (21). Also note that $V_C' = 0$ iff $I_C = 0$. Therefore, the function V_C is strictly Lyapunov at the DFE point according to the LaSalle's invariance principle [35] and hence E_0^C is globally asymptotically stable.

3.4 The Endemic Equilibrium Point (EEP) of the Model

The term "endemic", according to [36], refers to a disease affecting a number of people simultaneously, so as to show distinct connection with certain localities and is prevalent in that particular area(s) thereof. Mathematically, the EEP for our model was obtained by solving for all state variables while equating there derivatives with respect to time as zero. Basically, a model shall have an endemic equilibrium if the algebraic system derived from the model by setting all derivatives to zero, has a solution in which each state variable is strictly positive [37].

We define the EEP as $E_C^* = (S^*, I_C^*, R_C^*, V_C^*)$, a positive state solution of the model satisfying $\frac{dS}{dt} = \frac{dI_C}{dt} = \frac{dR_C}{dt} = \frac{dV_C}{dt} = 0$.

That is;

$$\frac{dS}{dt} = \Lambda - \nu_C S - \beta_C I_C S + \omega_C V_C + \theta_C R_C - \mu S = 0 \tag{23}$$

$$\frac{dI_C}{dt} = \beta_C I_C S - \gamma_C I_C - (\delta_C + \mu) I_C = 0 \tag{24}$$

$$\frac{dR_C}{dt} = \gamma_C I_C - \theta_C R_C - \mu R_C = 0 \tag{25}$$

$$\frac{dV_C}{dt} = \nu_C S - \omega_C V_C - \mu V_C = 0 \tag{26}$$

From (26),

$$V_C = \frac{\nu_C}{\omega_C + \mu} S \tag{27}$$

Similarly, from (24),

$$\begin{aligned} &\beta_C I_C S = (\gamma_C + \delta_C + \mu) I_C \\ &\implies S^* = \frac{(\gamma_C + \delta_C + \mu)}{\beta_C} > 0 \end{aligned} \tag{28}$$

By substituting (28) in (27), we have;

$$V_C^* = \frac{\nu_C(\gamma_C + \delta_C + \mu)}{\beta_C(\omega_C + \mu)} > 0. \tag{29}$$

Next, we add (23) to (26) together and obtain:

$$\Lambda - \mu S - (\delta_C + \mu) I_C - \mu R_C - \mu V_C = 0. \tag{30}$$

Substituting (28) and (29) in (30) yields;

$$\Lambda - \frac{\mu}{\beta_C}(\gamma_C + \delta_C + \mu) - (\delta_C + \mu)I_C - \mu R_C - \mu\frac{\nu_C(\gamma_C + \delta_C + \mu)}{\beta_C(\omega_C + \mu)} = 0. \tag{31}$$

Similarly, from (25), we have;

$$I_C = \frac{(\theta_C + \mu)}{\gamma_C}R_C. \tag{32}$$

Substituting (32) in (31), we have;

$$R_C = \frac{\Lambda - \frac{\mu}{\beta_C}(\gamma_C + \delta_C + \mu)(1 + \frac{\nu_C}{(\omega_C+\mu)})}{[\mu + \frac{(\delta_C+\mu)(\theta_C+\mu)}{\gamma_C}]}.$$

Now; $(1 + \frac{\nu_C}{(\omega_C+\mu)}) = \frac{(\mu+\omega_C+\nu_C)}{(\mu+\omega_C)} = \frac{1}{H}$ where $H = \frac{(\mu+\omega_C)}{(\mu+\omega_C+\nu_C)}$ from (18).

Also let $B = [\mu + \frac{(\delta_C+\mu)(\theta_C+\mu)}{\gamma_C}]$.

Therefore;

$$R_C^* = \frac{\Lambda - \frac{\mu}{H\beta_C}(\gamma_C + \delta_C + \mu)}{B} \qquad > 0 \tag{33}$$

if

$$[\Lambda - \frac{\mu}{H\beta_C}(\gamma_C + \delta_C + \mu)] \qquad > 0.$$

Finally, substituting (33) in (32), we obtain;

$$I_C^* = \frac{(\theta_C + \mu)}{B\gamma_C}[\Lambda - \frac{\mu}{H\beta_C}(\gamma_C + \delta_C + \mu)] \qquad > 0 \tag{34}$$

if

$$[\Lambda - \frac{\mu}{H\beta_C}(\gamma_C + \delta_C + \mu)] \qquad > 0$$

$$\implies \frac{\Lambda H\beta_C}{\mu(\gamma_C + \delta_C + \mu)} > 1. \tag{35}$$

Therefore, a unique endemic equilibrium point, $E_C^* = (S^*, I_C^*, R_C^*, V_C^*)$, for the COVID-19 model exists whenever $R_0^C = \frac{\Lambda H\beta_C}{\mu(\gamma_C+\delta_C+\mu)} > 1$. (Recall (21)).

3.5 Global Stability of the EEP

In order to analyze the global stability of the endemic equilibria of the model, we employed the Lyapunov method. A Lyapunov function is always positive and it is equal to zero only at the disease existing or endemic point of a model.

We defined an appropriate Lyapunov function for the COVID-19 model in (1) to (4) at the endemic equilibrium point $E_C^* = (S^*, I_C^*, R_C^*, V_C^*)$ as:

$$L_C(S, I_C, R_C.V_C) = \frac{1}{2}[(S - S^*) + (I_C - I_C^*) + (R_C - R_C^*) + (V_C - V_C^*)]^2 \tag{36}$$

Differentiating L_C wrt t,

$$\frac{dL_C}{dt} = [(S - S^*) + (I_C - I_C^*) + (R_C - R_C^*) + (V_C - V_C^*)] \times (\frac{dS}{dt} + \frac{dI_C}{dt} + \frac{dR_C}{dt} + \frac{dV_C}{dt})$$

$$= (N_C - N_C^*) \times \frac{dN_C}{dt}. \tag{37}$$

$N_C^* = S^* + I_C^* + R_C^* + V_C^*$

$= \frac{(\gamma_C+\delta_C+\mu)(\nu_C+\omega_C+\mu)}{\beta_C(\omega_C+\mu)} + I_C^*A_C$, where $I_C^* > 0$ and $A_C = (1 + \frac{\gamma_C}{(\theta_C+\mu)}) > 0$

Similarly, $\frac{(\gamma_C+\delta_C+\mu)(\nu_C+\omega_C+\mu)}{\beta_C(\omega_C+\mu)} = \frac{\Lambda}{\mu R_0^C}$, recall R_0^C from (21).
Substituting the above result in (37), we have;

$$\begin{aligned}\frac{dL_C}{dt} &= (N_C - (\frac{\Lambda}{\mu R_0^C} + I_C^* A_C)) \times (\Lambda - \mu N_C - \delta_C I_C) \\ &\leq (N_C - \frac{\Lambda}{\mu R_0^C}) \times (\Lambda - \mu N_C - \delta_C I_C) \\ &\leq (N_C - \frac{\Lambda}{\mu})(\Lambda - \mu N_C) \\ &\leq -\frac{(\Lambda - \mu N_C)^2}{\mu} \leq 0 \end{aligned} \tag{38}$$

Since $I_C > 0$ and $R_0^C > 1$ at E_C^*.
Therefore, for $R_0^C > 1$, the endemic equilibrium point E_C^* exists and the function L_C is strictly Lyapunov function. This implies that E_C^* is globally asymptotically stable.

3.6 Sensitivity Analysis of R_e

In order to obtain the effect of each parameter affecting the effective reproduction number on the disease transmission and control, we performed there sensitivity analyses. This analysis helps to determine whether a parameter has positive or negative impact on the continued transmission of the disease. We defined the normalized forward sensitivity index of R_e with respect to a parameter p as [32, 38];

$$\begin{aligned}\Gamma_p^{R_e} &= \frac{\partial R_e}{R_e} \div \frac{\partial p}{p} \\ &= \frac{\partial R_e}{\partial p} \times \frac{p}{R_e}\end{aligned}$$

Since R_e is the product of R_0^C with a constant non-zero value, it suffices to say that:

$$\Gamma_p^{R_0^C} = \frac{\partial R_0^C}{\partial p} \times \frac{p}{R_0^C} \tag{39}$$

We recall from (21) that,

$$R_0^C = \frac{\Lambda\beta_C(\mu+\omega_C)}{\mu(\mu+\omega_C+\nu_C)(\gamma_C+\delta_C+\mu)} \tag{40}$$

For parameter Λ,

$$\begin{aligned}\Gamma_\Lambda^{R_0^C} &= \frac{\partial R_0^C}{\partial \Lambda} \times \frac{\Lambda}{R_0^C} \\ &= \frac{\beta_C(\mu+\omega_C)}{\mu(\mu+\omega_C+\nu_C)(\gamma_C+\delta_C+\mu)} \times \frac{\Lambda}{R_0^C} \\ &= \frac{R_0^C}{\Lambda} \times \frac{\Lambda}{R_0^C} = 1\end{aligned}$$

For β_C,

$$\begin{aligned}\Gamma_{\beta_C}^{R_0^C} &= \frac{\partial R_0^C}{\partial \beta_C} \times \frac{\beta_C}{R_0^C} \\ &= \frac{\Lambda(\mu+\omega_C)}{\mu(\mu+\omega_C+\nu_C)(\gamma_C+\delta_C+\mu)} \times \frac{\beta_C}{R_0^C}\end{aligned}$$

$$= \frac{R_0^C}{\beta_C} \times \frac{\beta_C}{R_0^C} = 1$$

For μ,

$$\Gamma_{\mu}^{R_0^C} = \frac{\partial R_0^C}{\partial \mu} \times \frac{\mu}{R_0^C}$$

$$\frac{\partial R_0^C}{\partial \mu} = \Lambda\beta_C \times \frac{\partial B}{\partial \mu} \tag{41}$$

Where $B = \frac{(\mu+\omega_C)}{(\mu^2+\mu\omega_C+\mu\nu_C)(\mu+\delta_C+\gamma_C)}$

Using quotient and product rules of differentiation, we obtained,

$$\frac{\partial B}{\partial \mu} = \frac{V - (\mu+\omega_C)[\mu(\mu+\omega_C+\nu_C) + (\mu+\delta_C+\gamma_C)(2\mu+\omega_C+\nu_C)]}{V^2}$$

Where $V = (\mu^2 + \mu\omega_C + \mu\nu_C)(\mu + \delta_C + \gamma_C)$

Substituting the above in (41), we have;

$$\Gamma_{\mu}^{R_0^C} = \Lambda\beta_C \times \frac{\partial B}{\partial \mu} \times \frac{\mu}{R_0^C}$$

$$= R_0^C \times \frac{V}{(\mu+\omega_C)} \times \frac{\partial B}{\partial \mu} \times \frac{\mu}{R_0^C}$$

$$= \frac{\mu}{(\mu+\omega_C)} \times \frac{V - (\mu+\omega_C)[\mu(\mu+\omega_C+\nu_C) + (\mu+\delta_C+\gamma_C)(2\mu+\omega_C+\nu_C)]}{V}$$

For ω_C,

$$\Gamma_{\omega_C}^{R_0^C} = \frac{\partial R_0^C}{\partial \omega_C} \times \frac{\omega_C}{R_0^C}$$

$$\frac{\partial R_0^C}{\partial \omega_C} = \frac{\Lambda\beta_C}{\mu(\gamma_C+\delta_C+\mu)} \times \frac{\partial B}{\partial \omega_C} \tag{42}$$

Where $B = \frac{\mu+\omega_C}{\mu+\omega_C+\nu_C}$

Using quotient rule of differentiation, we obtained,

$$\frac{\partial B}{\partial \omega_C} = \frac{\nu_C}{(\mu+\omega_C+\nu_C)^2}$$

Substituting the above in (42), we have;

$$\Gamma_{\omega_C}^{R_0^C} = \frac{\omega_C\nu_C}{(\mu+\omega_C)(\mu+\omega_C+\nu_C)}$$

For ν_C,

$$\Gamma_{\nu_C}^{R_0^C} = \frac{\partial R_0^C}{\partial \nu_C} \times \frac{\nu_C}{R_0^C}$$

$$\frac{\partial R_0^C}{\partial \nu_C} = \frac{\Lambda\beta_C}{\mu(\gamma_C+\delta_C+\mu)} \times \frac{\partial B}{\partial \nu_C} \tag{43}$$

Where $B = \frac{1}{\mu+\omega_C+\nu_C}$

Using quotient rule of differentiation, we obtained,

$$\frac{\partial B}{\partial \nu_C} = -(\mu+\omega_C+\nu_C)^{-2}$$

Substituting the above in (43), we have;

$$\Gamma_{\nu_C}^{R_0^C} = \frac{-\nu_C}{(\mu + \omega_C + \nu_C)}$$

For γ_C,

$$\Gamma_{\gamma_C}^{R_0^C} = \frac{\partial R_0^C}{\partial \gamma_C} \times \frac{\gamma_C}{R_0^C}$$

$$\frac{\partial R_0^C}{\partial \gamma_C} = \frac{\Lambda \beta_C}{\mu(\mu + \omega_C + \nu_C)} \times \frac{\partial B}{\partial \gamma_C} \tag{44}$$

Where $B = \frac{1}{(\gamma_C + \delta_C + \mu)}$

Using quotient rule of differentiation, we obtained,

$$\frac{\partial B}{\partial \gamma_C} = -(\gamma_C + \delta_C + \mu)^{-2}$$

Substituting the above in (44), we have;

$$\Gamma_{\gamma_C}^{R_0^C} = \frac{-\gamma_C}{(\gamma_C + \delta_C + \mu)}$$

Lastly, for δ_C,

$$\Gamma_{\delta_C}^{R_0^C} = \frac{\partial R_0^C}{\partial \delta_C} \times \frac{\delta_C}{R_0^C}$$

$$\frac{\partial R_0^C}{\partial \delta_C} = \frac{\Lambda \beta_C}{\mu(\mu + \omega_C + \nu_C)} \times \frac{\partial B}{\partial \delta_C} \tag{45}$$

Where $B = \frac{1}{(\gamma_C + \delta_C + \mu)}$

Using quotient rule of differentiation, we obtained,

$$\frac{\partial B}{\partial \delta_C} = -(\gamma_C + \delta_C + \mu)^{-2}$$

Substituting the above in (45), we have;

$$\Gamma_{\delta_C}^{R_0^C} = \frac{-\delta_C}{(\gamma_C + \delta_C + \mu)}$$

Therefore, by substituting the values of the parameters in table 2 into the seven sensitivity indices above, we obtain table 3 below:

Table 3: Sensitivity Indices for the Basic Reproduction Number

Parameters	Signs	Values
Λ	+	1
β_C	+	1
ω_C	+	0.1978857
ν_C	-	0.9540073
γ_C	-	0.97814180
δ_C	-	0.0210713
μ	-	0.2446653

Interpretation of Table

A positive sensitivity index implies that an increase in the value of such parameter by some percentage will increase the value of R_0 by some percentage corresponding to the value of the index and vice versa. For example, an increase in the value of ω_C by 10% will increase R_0 by 1.97% while an increase in the value of ν_C by 10% will decrease R_0 by 9.54%.

4 Numerical Simulations

Numerical solution of the model was obtained by employing the fourth order Runge Kutta method on MATLAB subroutine, using the parameter values in table 2 over a period of 30 weeks with step size 1. The initial conditions of the state variables are; $S(0) = 300$, $I_C(0) = 5$, $R_C(0) = 0$ and $V_C(0) = 0$.

Figure 4 shows the simulation of the susceptible population. This class experiences a rapid decline in its size over a period of 7 weeks as its members got infected with COVID-19 and move to the infected class as shown in figure 5. After this time, however, the susceptible class maintained a size of about 50 throughout the simulation owning to the fact that there is a steady outflow of its members into the infected and vaccinated classes and inflow from the recovered and vaccinated classes via the factors of disease relapse and immunity wane respectively.

The infected population experiences a rapid increase in size for about 4 weeks and then a continuous decrease up until the 20th week during which it approaches zero. The decline in the size of this population is strongly associated with the efficacy of treatment resulting in the corresponding increase experienced by the recovered class as indicated in figure 6. After about 13 weeks, however, the recovered class experienced a slight decrease in size signifying that although people continue to recover, some who have recovered experience a relapse and are moved back to the susceptible class. The vaccinated population in figure 7 experiences a rapid increase in its size for the first 5 weeks and then a slow increase for the entire period of the simulation as people continue to move into this class from the susceptible class. This increase is slow because of the effect of immunity wane on this class as some of its members return to being susceptible.

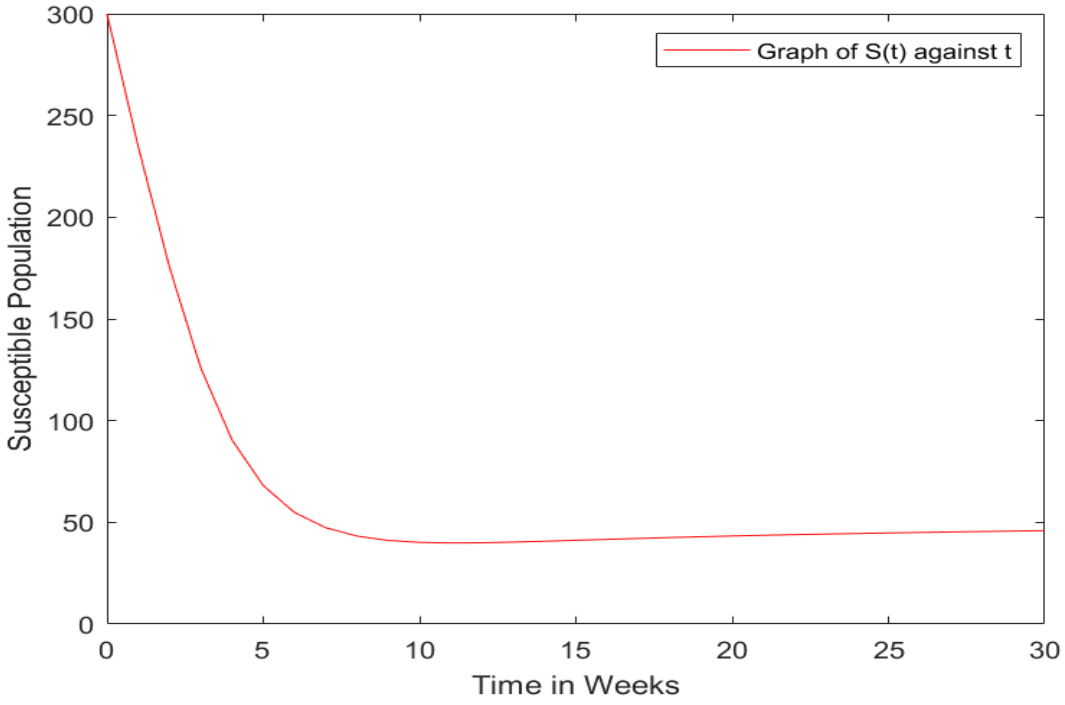

Figure 4: Susceptible COVID-19 Population against Time

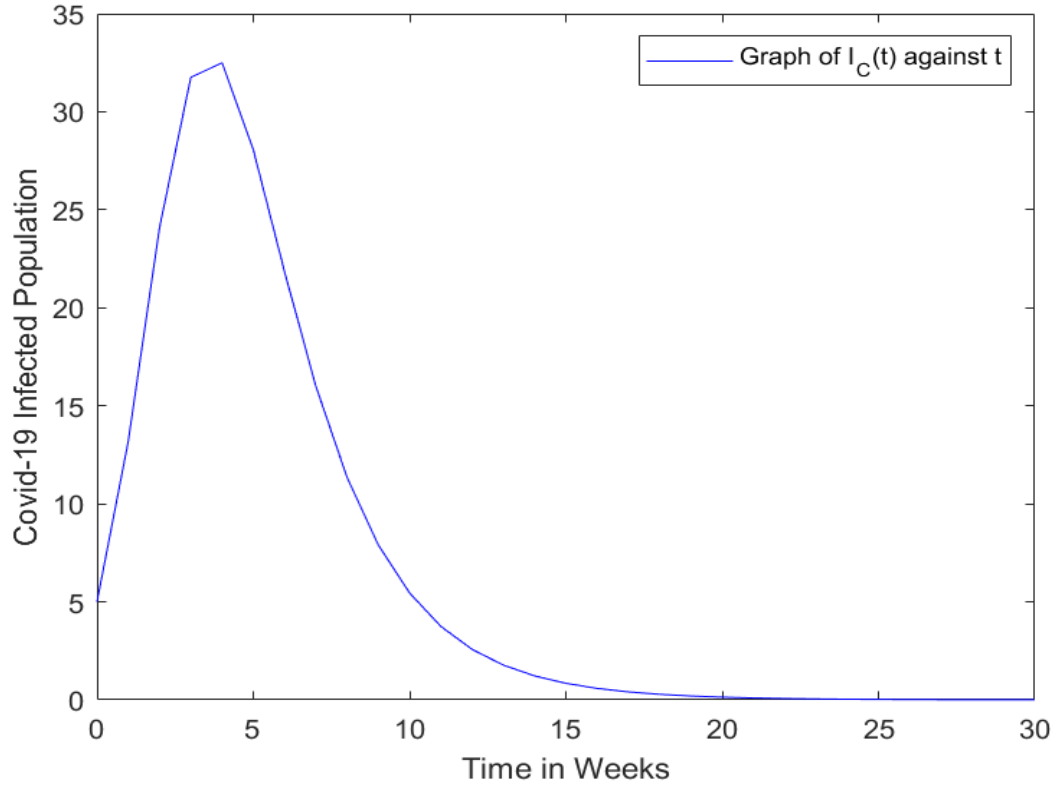

Figure 5: COVID-19 Infected Population against Time

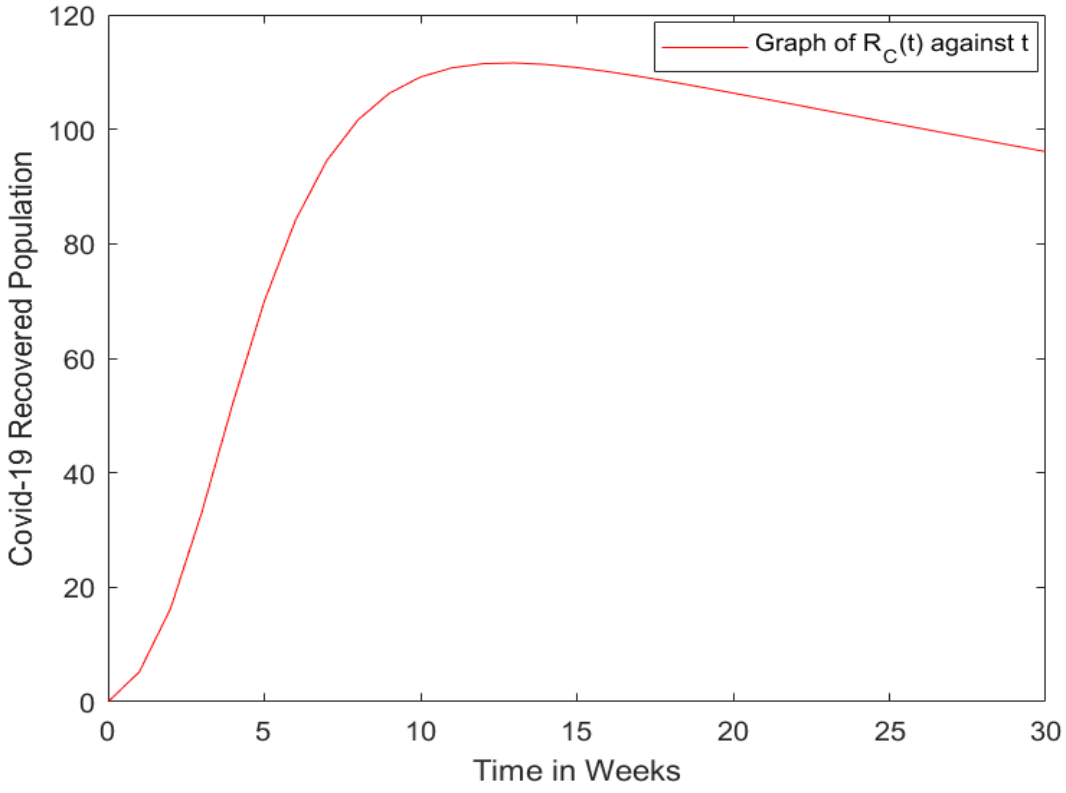

Figure 6: COVID-19 Recovered Population against Time

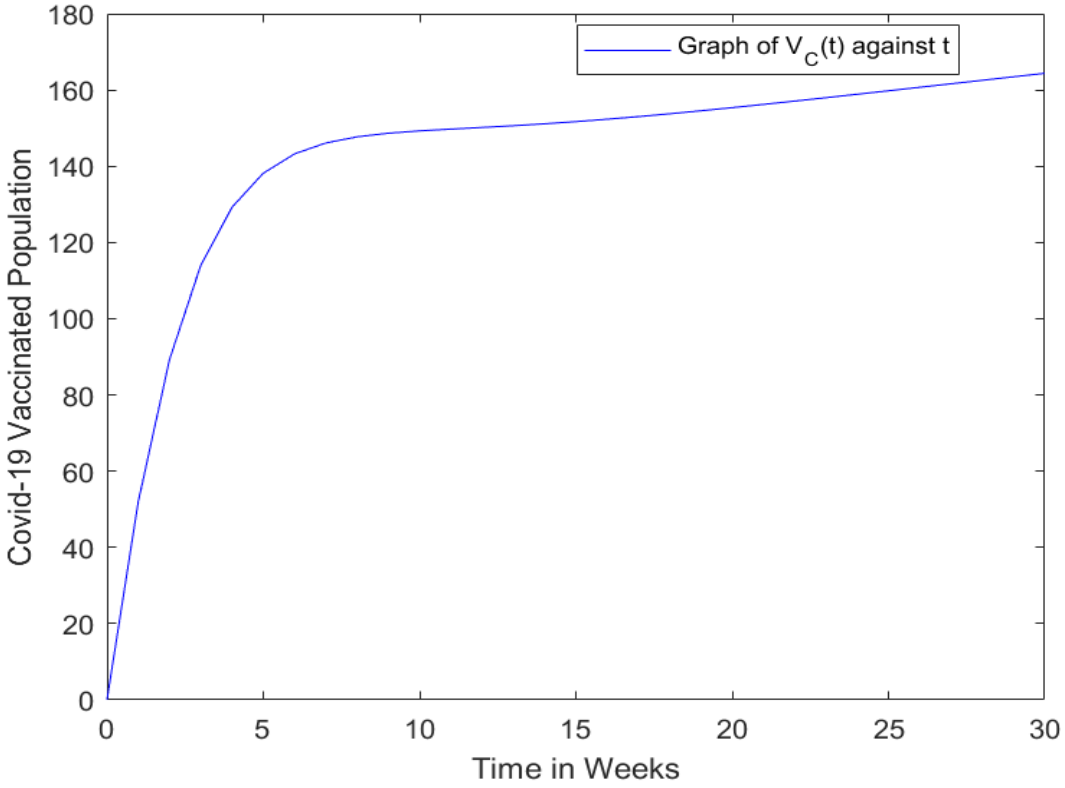

Figure 7: COVID-19 Vaccinated Population against Time

4.1 Numerical Simulation and Variation of the Model's Parameters

Figure 8 shows the effect of varying the vaccination rate, ν_C, on the infected and vaccinated populations. By increasing ν_C, it is observed that the disease not only dies out faster but also has a reduced peak level of infectiousness as seen in figure 8a. On the contrary, increasing ν_C yields an increase in the peak value of the vaccinated class, indicated by figure 8b. Increasing the treatment rate of COVID-19, γ_C, yields a significant reduction in the infected class and a shorter time of infectiousness, shown in figure 9. The recovered class, on the other hand experienced an increase in its population with increase in γ_C, as indicated in figure 9b.

An increase in the rate of disease relapse, shown in figure 10, results in a significant decrease in the recovered population and increase in the susceptible population which in turn results in an increase of the infected population and the peak of infectiousness. Similarly, increasing the value of the rate of immunity wane after vaccination, shown in figure 11, results in an increase of the susceptible and infected populations and decrease in the vaccinated population. Figure 12 shows the effect of increasing the contact rate, β_C, indicating a decline in the susceptible population and corresponding progression into the infected population. The vaccination class in figure 12c is seen to experience a decrease in its population as β_C increases. Increasing the value of the recruitment rate, Λ results in a simultaneous increase in the susceptible and infected classes as shown in figure 13.

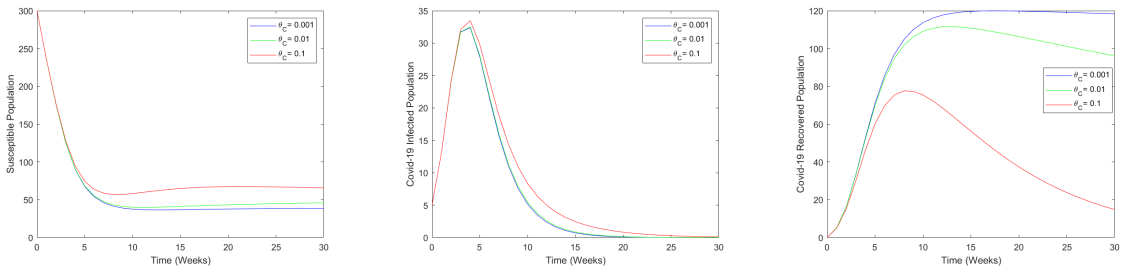

(a) Susceptible profile (b) Infected Profile (c) Recovered Profile

Figure 10: Effects of Disease Relapse

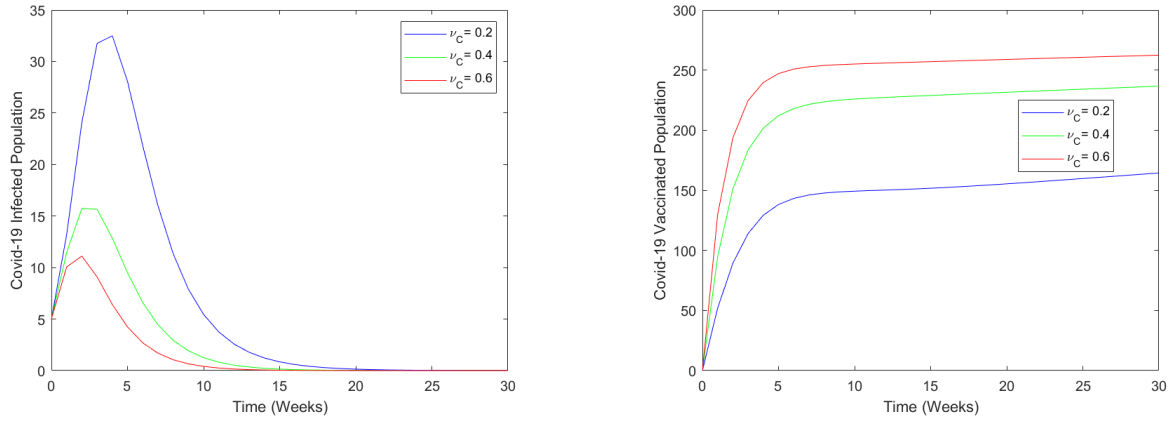

(a) Infected profile (b) Vaccinated Profile

Figure 8: Effects of Vaccination Rate

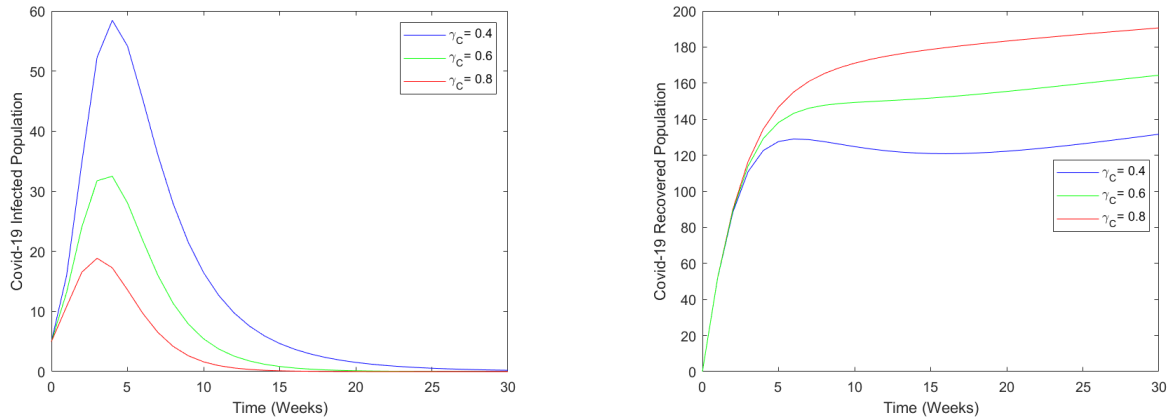

(a) Infected profile (b) Recovered Profile

Figure 9: Effects of Treatment Rate

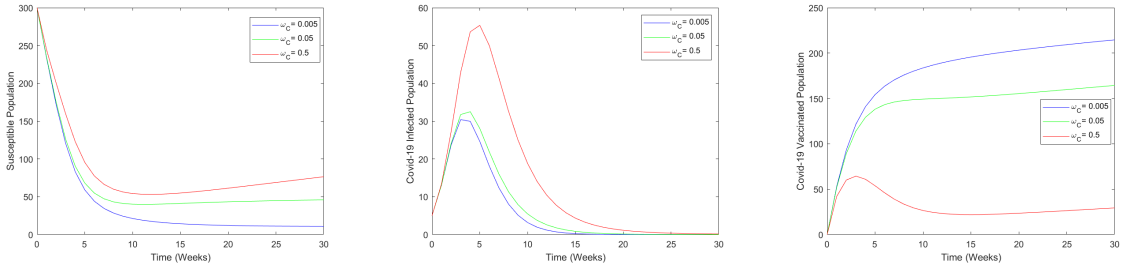

(a) Susceptible profile (b) Infected Profile (c) Vaccinated Profile

Figure 11: Effects of Immunity Wane after Vaccination

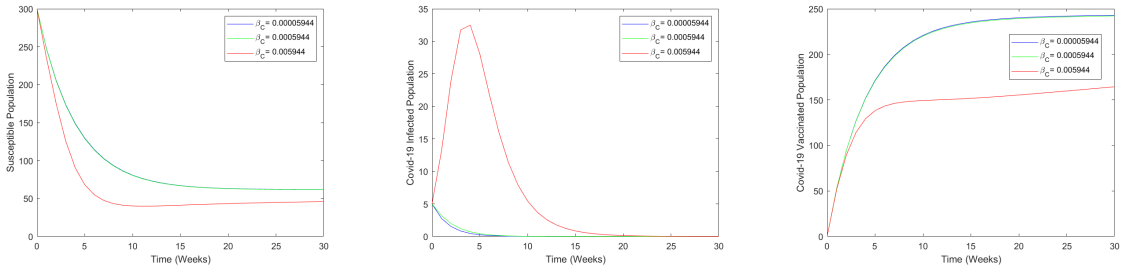

(a) Susceptible profile (b) Infected Profile (c) Vaccinated Profile

Figure 12: Effects of COVID-19 Contact Rate

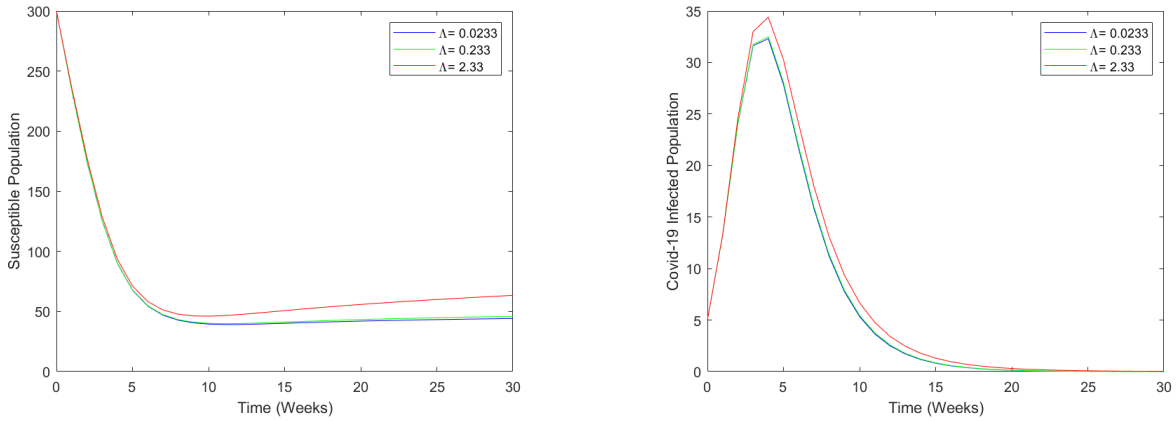

(a) Susceptible profile (b) Infected Profile

Figure 13: Effects of Recruitment rate into the Susceptible population

5 Conclusion and Recommendation

Although various mathematical models have been employed to study the spread of COVID-19 in Nigeria, with focus on active cases and mortality, limited attention has been given to the effects of disease relapse following recovery and the waning of immunity after vaccination. This research work presents a novel deterministic model for the transmission and control dynamics of COVID-19, with significant emphasis on re-infection and immunity waning post vaccination, fitted with data from Nigeria.

The model was established to be epidemiologically and mathematically well posed, suitable to represent the real life scenario being described. Results of the stability analyses of the model shows existence of a stable disease free equilibrium point for COVID-19 whenever the effective reproduction number is

less than unity, $R_e < 1$, indicating that the studied population can remain in the absence of the disease if necessary implementations are made and parameter values controlled. Sensitivity analysis of R_e shows that recruitment and transmission rates are the most sensitive parameter to increase the spread of the disease, followed by the rate of loss of immunity while vaccination and treatment rates are the most sensitive parameter to decrease its spread.

It is therefore pertinent that awareness and sensitization campaigns be intensified, especially to people living in rural and COVID-19 endemic areas, on how to reduce disease transmission via proper hygiene and environmental cleanliness such as avoiding overcrowded areas with poor ventilation, washing of hands under running water, social distancing, coughing/sneezing into the elbow etc. This will result in a significant reduction of contact/transmission rates and thus prevent both cases of infection and re-infection with the diseases thereby also reducing the rate of disease relapse. Moreover, we advocate that point of care diagnosis (POCD) be made available in endemic populations. This will enable quick, easily accessible and accurate diagnosis of the disease, followed by efficacious treatment. Although, several vaccines have been developed for COVID-19, we besiege the health institutions to intensify research on the emergence of a vaccine with 100% efficacy against the infection as this will put a complete end to cases of waning immunity. To the scientific world, we recommend that an optimal control application with cost effectiveness analysis be made on the developed model in order to see what parameter or combination of parameters will yield the optimum control to the disease while also minimizing cost.

Acknowledgments

The authors acknowledge with gratitude the support of the Mathematical Sciences Department of the Federal University of Technology, Akure and the Library at Ofin Chambers, Ibadan for providing conducive for learning and research environments during this research.

References

[1] Brauer, F. (2017). Mathematical epidemiology: Past, present, and future. Infectious Disease Modelling 2(2), 113–127.

[2] McEvedy, C. (1988). The bubonic plague. Scientific American 258 (2), 118–123.

[3] Guan, W. J., Ni, Z. Y., Hu, Y., Liang, W. H., Ou, C. Q. et al. (2020). Clinical characteristics of coronavirus disease 2019 in china. New England journal of medicine 382 (18), 1708–1720.

[4] Tamblyn, S., Salvadori, M., St-Louis, P., Yeung, T., Haroon, B. et al. (2020). Clinical management of patients with moderate to severe covid-19-interim guidance. Public Heal Agency Canada, 1–20.

[5] Cascella, M., Rajnik, M., Aleem, A., Dulebohn, S. C., Di Napoli, R. (2020). Features, evaluation, and treatment of coronavirus (covid-19). Statpearls publishing, Treasure Island (FL) PMID: 32150360.

[6] World Health Organization (2024). Covid-19 epidemiological update, 19 January 2024.

[7] Cucinotta, D. and Vanelli, M. (2020). WHO declares covid-19 a pandemic. Acta bio medica: Atenei parmensis 91 (1), 157.

[8] Adeosun M. E., Akin-Awoniran, B. O. and Akingbade, J. A. (2022). A novel mathematical model for curbing the spread of covid-19 in nigeria. International Journal of Mathematics Trends and Technology-IJMTT 68, 510–522.

[9] World Health Organization (2023). Clinical management of covid-19: living guideline, 13 january 2023. Tech. rep., WHO.

[10] Odunayo, B. J., Nnamdi, E. and Correa, F. M. (2025). Initial Growth Rate and Model Performance for COVID-19 in Nigeria. Contemporary Mathematics, 2377–2391.

[11] Nigerian centre for Disease Control and Prevention (NCDC), COVID-19 Nigeria, https://covid19.ncdc.gov.ng/, last accessed 2024/07/21.

[12] World Health Organization (WHO), Number of COVID-19 cases reported to WHO, https://data.who.int/dashboards/covid19/cases?n=c, last accessed 2024/01/24.

[13] Worldometers, COVID-19 CORONAVIRUS PANDEMIC Weekly Trends, https://www.worldometers.info/coronavirus/, last accessed 2024/07/11.

[14] Baba, B. A. and Bilgehan, B. (2021). Optimal control of a fractional order model for the covid-19 pandemic. Chaos, Solitons & Fractals 144, 1–12.

[15] Khajji B., Kouidere, A., Elhia, M., Balatif, O. and Rachik, M. (2021). Fractional optimal control problem for an age-structured model of covid-19 transmission. Chaos, Solitons & Fractals 143, 1–15.

[16] Ren, X., Zhou, J., Guo, J., Hao, C., Zheng, M. et al. (2022). Reinfection in patients with covid-19: a systematic review. Global Health Research and Policy 7 (1), 1–20.

[17] Shah, K., Abdeljawad, T., Mahariq, I. and Jarad, F. (2020). Qualitative analysis of a mathematical model in the time of covid-19. BioMed Research International, 1–11.

[18] Zeb, A., Alzahrani, E., Erturk, V. S. and Zaman, G. (2020). Mathematical model for coronavirus disease 2019 (covid-19) containing isolation class. BioMed research international, 1–7.

[19] Bentout, S., Chekroun, A. and Kuniya, T. (2020). Parameter estimation and prediction for coronavirus disease outbreak 2019 (covid-19) in algeria. AIMS Public Health 7 (2), 1–13.

[20] Panwar, V. S., Uduman, P. S. and Gómez-Aguilar, J. F. (2021). Mathematical modeling of coronavirus disease covid-19 dynamics using cf and abc non-singular fractional derivatives. Chaos, Solitons & Fractals 145, 1–14.

[21] Sun, T. and Wang, Y. (2020). Modeling covid-19 epidemic in heilongjiang province, china. Chaos, Solitons & Fractals 138, 1–6.

[22] Ndaïrou, F., Area, I., Nieto, J. J. and Torres, D. F. (2020). Mathematical modeling of covid-19 transmission dynamics with a case study of wuhan. Chaos, Solitons & Fractals 135, 1–7.

[23] Kumar, P., Erturk, V. S., Abboubakar, H. and Nisar, K. S. (2021). Prediction studies of the epidemic peak of coronavirus disease in brazil via new generalised caputo type fractional derivatives. Alexandria Engineering Journal 60 (3), 3189–3204.

[24] Faniran, T. S., Ali, A., Al-Hazmi, N. E., Asamoah, J. K., Nofal, T. A. and Adewole, M. O. (2022). New variant of sars-cov-2 dynamics with imperfect vaccine. Complexity, 1–17.

[25] Baba, I. A., Yusuf, A., Nisar, K. S., Abdel-Aty, A.-H. and Nofal, T. A. (2021). Mathematical model to assess the imposition of lockdown during covid-19 pandemic. Results in Physics 20, 1–7.

[26] Adewole, M. O., Onifade, A. A., Abdullah, F. A., Kasali, F. and Ismail, A. I. (2021). Modeling the dynamics of covid-19 in nigeria. International journal of applied and computational mathematics 7, 1–25.

[27] Tilahun, G. T., Makinde, O. D. and Malonza, D. (2018). Co-dynamics of pneumonia and typhoid fever diseases with cost effective optimal control analysis. Applied Mathematics and Computation 316, 438–459.

[28] Macrotrends, Nigeria Life Expectancy 1950-2024, https://www.macrotrends.net/global-metrics/countries/NGA/nigeria/life-expectancy, last accessed 2024/07/11.

[29] Lenhart, S. and Workman, J. T. (2007). Optimal control applied to biological models. Crc Press, Chapman and Hall/CRC.

[30] Akinade, M. O., Afolabi, A. S. and Kimathi, M. E. (2019). Mathematical modeling and stability analyses of lassa fever disease with the introduction of the carrier compartment. Mathematical Theory and Modeling 9 (6), 45–62.

[31] Ogunmodimu, M. O., Enock, E. P., Kenyatta, A. P., Affognon, S. B. and Onwuegbuche, F. C. (2024). A mathematical model for the prevention of hiv/aids in the presence of undetectable equals untransmittable viral load. International Journal of Mathematical Sciences and Optimization: Theory and Applications 10 (2), 36–57.

[32] Akinade, M. O. and Afolabi, A. S. (2020). Sensitivity and stability analyses of a lassa fever disease model with control strategies. IOSR Journal of Mathematics (IOSR-JM) 16 (1), 29–42.

[33] Danbaba, U., Aloko, M. and Ayinde, A. (2024). Mathematical modeling of mosquito borne diseases with vertical transmissions as applied to dengue. International Journal of Mathematical Sciences and Optimization: Theory and Applications 10 (3), 31–56.

[34] Yusuf, T. T. (2021). On global stability of disease-free equilibrium in epidemiological models. European Journal of Mathematics and Statistics 2 (3), 37–42.

[35] La Salle, J. P. (1976). The stability of dynamical systems. Society for Industrial and Applied Mathematics.

[36] Stevenson, A. (2010). Oxford dictionary of English. Oxford University Press, USA.

[37] Brown, C. W., Novotni, D., Weber, A. et al. (2006). Algorithmic methods for investigating equilibria in epidemic modeling. Journal of Symbolic Computation 41 (11), 1157–1173.

[38] Bandekar, S. R. and Ghosh, M. (2022). A co-infection model on tb-covid-19 with optimal control and sensitivity analysis. Mathematics and Computers in Simulation 200, 1–31.